Bull Volcanol (1996) 58:5–18

ORIGINAL PAPER

L. Keszthelyi · R. Denlinger

The initial cooling of pahoehoe flow lobes

Received: 26 November 1994 / Accepted: 1 December 1995

Abstract In this paper we describe a new thermal model for the initial cooling of pahoehoe lava flows. The accurate modeling of this initial cooling is important for understanding the formation of the distinctive surface textures on pahoehoe lava flows as well as being the first step in modeling such key pahoehoe emplacement processes as lava flow inflation and lava tube formation. This model is constructed from the physical phenomena observed to control the initial cooling of pahoehoe flows and is not an empirical fit to field data. We find that the only significant processes are (a) heat loss by thermal radiation, (b) heat loss by atmospheric convection, (c) heat transport within the flow by conduction with temperature and porosity-dependent thermal properties, and (d) the release of latent heat during crystallization. The numerical model is better able to reproduce field measurements made in Hawai'i between 1989 and 1993 than other published thermal models. By adjusting one parameter at a time, the effect of each of the input parameters on the cooling rate was determined. We show that: (a) the surfaces of porous flows cool more quickly than the surfaces of dense flows, (b) the surface cooling is very sensitive to the efficiency of atmospheric convective cooling, and (c) changes in the glass forming tendency of the lava may have observable petrographic and thermal signatures. These model results provide a quantitative explanation for the recently observed relationship between the surface cooling rate of pahoehoe lobes and the porosity of those lobes (Jones 1992, 1993). The predicted sensitivity of cooling to atmospheric convection suggests a simple field experiment for verification, and the model provides a tool to begin studies of the dynamic crystallization of real lavas. Future versions of the model can also be made applicable to extraterrestrial, submarine, silicic, and pyroclastic flows.

Key words Lava · Cooling · Pahoehoe · Hawai'i

Editorial responsibility: S. Carey

Laszlo Keszthelyi (✉) · Roger Denlinger
Hawaiian Volcano Observatory,
United States Geological Survey, P.O. Box 51,
Hawaii Volcanoes National Park, HI 96718, USA

Laszlo Keszthelyi
Hawaii Institute for Geophysics and Planetology, SOEST,
2525 Correa Road, Honolulu, HI 96822, USA
Fax: +808–967–8890
E-mail: lpk@soest.hawaii.edu

Introduction

Pahoehoe lava flows are a major component of basaltic volcanism which, in turn, forms most of the surfaces of the Earth and the other terrestrial planets. Essentially all observed submarine lava flows can be classified as variants of one of the various subaerial forms of pahoehoe (e.g., Ballard et al. 1979; BVSP 1981; Appelgate and Embley 1992; Bryan et al. 1994). It has also been argued that continental flood basalt flow units are inflated pahoehoe sheet flows (e.g., Hon and Kauahikaua 1991; Self et al. 1991). Pahoehoe flows may also have been detected on Mars (Theilig and Greeley 1986) and Venus (Bruno et al. 1992). In Hawai'i, pahoehoe flows cover approximately 86% of Kilauea Volcano (Holcomb 1987) and 50% of Mauna Loa (Lockwood and Lipman 1987).

This paper examines the initial few minutes of the cooling of pahoehoe lava flow lobes. This initial cooling is of interest for three reasons. Firstly, the distinctive millimeter- to centimeter-scale pahoehoe surface textures form in this time. Secondly, the growth of pahoehoe lobes is controlled largely by the temperature-dependent rheology of the glassy skin that forms on this time scale. Thirdly, understanding the cooling of pahoehoe flows on the time scale of seconds and minutes is an important first step in understanding their cooling over longer time scales.

A wealth of field data has been collected recently on the cooling of pahoehoe flows on the Pu'u 'O'o–Kupaianaha flow field on Kilauea Volcano. These field

data include temperature measurements using radiometers (Jones 1992, 1993), a spectroradiometer (Flynn and Mouginis-Mark 1992), and thermocouples (Hon et al. 1994a, b; Keszthelyi and Denlinger, this study). In related work Wilmoth and Walker (1993) measured the growth of the chill crust on flow lobes, and there have been attempts to make in situ measurements of the rheology of the skin on these Kilauea lavas (S. Rowland, pers. comm. 1991; Keszthelyi 1994a).

Despite the importance of pahoehoe lava flows and the wealth of field data from them, only a few lava flow cooling studies investigate conditions appropriate for pahoehoe flows. The thermal model presented in Head and Wilson (1986) and Wilson and Head (1994) would appear to be directly applicable to pahoehoe lava flows, but we will show that their model uses inappropriate approximations that lead to inaccurate estimates. For time scales of hours to days, Hon et al. (1994a) were able to accurately fit observed cooling rates with empirical cooling curves, but it is not straightforward to use their results for other than subaerial Hawaiian pahoehoe flows. The work most similar to that presented here is the numerical model accompanying the wax modeling of lava flows by Griffiths and Fink (1992a, b). Other models, such as Crisp and Baloga (1990, 1994) and Pinkerton and Wilson (1994), make assumptions appropriate for channelized or 'a'a flows, but not pahoehoe lobes (e.g., well-mixed flow interiors).

Even the most recent theoretical cooling models for lava flows have not included the effect of vesicles or temperature-dependent thermal properties. This is despite laboratory data (e.g., Birch and Clark 1940; Murase and McBirney 1973; Robertson and Peck 1974), thermal models for dikes (e.g., Delaney 1988; Carrigan et al. 1992), thermal models for lava lakes (e.g., Peck 1978; Hardee 1980), field observations (Jones 1992, 1993), and theoretical calculations (Keszthelyi 1994b), which all suggest that these effects are important.

The main goal of this paper is to present a new thermal model that accurately describes the initial cooling of pahoehoe lava flows. We first discuss observations of active pahoehoe flow lobes and the physical processes which play a role in their cooling. The significant processes are then quantified and the key parameters are constrained using published laboratory data and field measurements. The resulting set of equations is used to construct a numerical model which is tested using field data collected by ourselves and others. We also compare our model to previous lava flow cooling models and determine the sensitivity of our model to each of the input parameters. We end by discussing future applications of the model and the new field experiments that it suggests.

Observations of active pahoehoe flow lobes

The term pahoehoe covers a wide range of lava flow types, from classic entrail and ropy pahoehoe to lavas transitional to 'a'a, such as slabby and toothpaste pahoehoe. In this study we concentrate on pahoehoe lobes with smooth surfaces, but our conclusions should also apply, at least qualitatively, to other forms of pahoehoe.

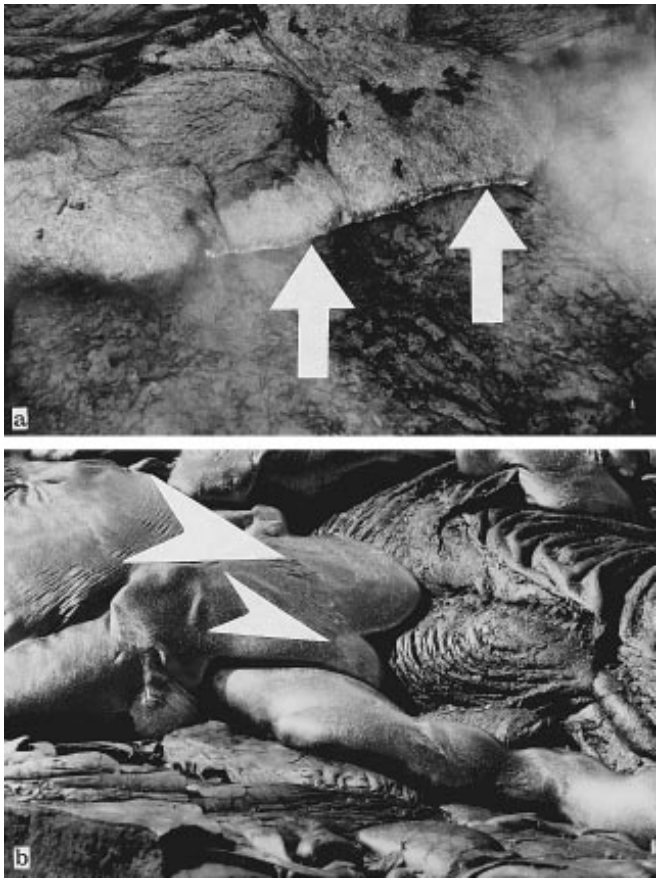

Fig. 1a, b Photographs of active Hawaiian pahoehoe flow lobes. **a** Red lava is exposed only at front of lobe, producing the incandescent lip (*arrows*). The *darker pieces* on top of the lobe are parts of the underlying surface that the active lobe has picked up. **b** Red lava is exposed where the two indicated breakouts started and the chill crust is carried forward along with the flow. The lobe in **a** was advancing at only approximately 0.5 cm/s, whereas the lobe in **b** moved at approximately 3 cm/s. In both cases the lobes are approximately 30 cm tall and 1 m wide and grew much like inflating balloons underneath their flexible skins of chilled lava

Pahoehoe lobes are typically 20–300 cm wide, 10–50 cm thick, and advance at millimeters to tens of centimeters per second (Fig. 1). These small lobes can coalesce to form sheets many tens of meters in width and hundreds of meters in length. The pahoehoe lobes continue to inflate even after a thick, brittle crust has formed, converting the <50-cm-thick lobes into 3- to 5-m-thick sheets or tumuli (Mattox et al. 1993; Hon et al. 1994a). Lava tubes that form in these inflated flows provide the insulation needed to transport the lava from the vent to the small pahoehoe lobes.

Individual lobes advance as inflating, fluid-filled balloons within a stretching skin of chilled lava. The size, shape, and direction and speed of advance of lobes are

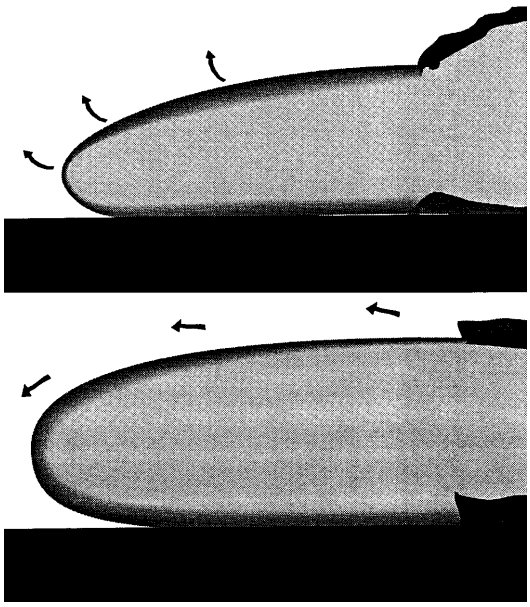

Fig. 2 Cross section of two end-member pahoehoe flow lobes. Sketch shows the two end members of flow lobe motion shown in Fig. 1. In the first, slow-moving case, the lobe grows by pushing the crust up and out of the way of the lobe front. The thickness of the crust increases back toward the initial breakout point. In the faster-moving case, the crust is carried along the top of the lobe and then rolled under the lobe front. Here the crust thickens toward the front of the lobe. Various combinations of these two end-members are common

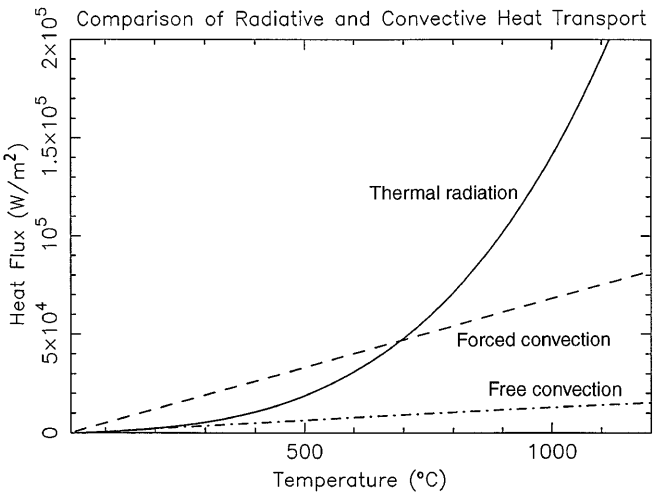

Fig. 3 Comparison of radiative and convective heat loss from pahoehoe lobes. Plot shows heat loss at the surface of a lobe by thermal radiation, forced atmospheric convection, and free atmospheric convection as a function of surface temperature. A heat transfer coefficient of 70 W/m^2 K was used for forced convection and free convection varies with surface temperature, but is generally approximately 11 W/m^2 K. Note that at a surface temperature of 700 °C forced convection (cooling by the wind) becomes the dominant heat loss mechanism

controlled by a complex interplay between the rheology of the skin, rheology of the molten interior of the lobe, centimeter-scale topography, local volumetric flux, and the geometry of the crack the lava is extruded from. Each of these parameters depend on many other variables such as cooling rate, lava composition, vesicularity of the lava, hydrostatic pressure driving the flow, etc. Previous workers have noted the key role volumetric flux plays in determining the morphology of a lava flow. Pahoehoe lobes (and pillow lavas) form at the low volumetric flux end of the spectrum of lava flows (e.g., Griffiths and Fink 1992a; Gregg and Fink 1995). At higher flow rates a continuous skin does not form and the lobe transitions to a channelized flow.

During the initial emplacement of pahoehoe flow lobes, most of the motion is accommodated by stretching of the plastic chilled skin. The stretching is concentrated along a tear in the skin and is usually the only area in which incandescent lava is exposed. The cooling we refer to in this paper starts at this tear. Depending on several factors, of which flow velocity seems dominant, the tear in the crust can be located on different parts of the lobe (Figs. 1 and 2). An accurate cooling model, combined with a temperature-dependent rheology for the chilled glassy skin, is the first step in understanding the details of the flow dynamics of pahoehoe flow lobes. By understanding the behavior of pahoehoe lobes in this level of detail, we hope to eventually better explain other aspects of these flows, such as the differences in vesicle distributions (Walker 1989; Wilmoth and Walker 1993), surface textures (e.g., Rowland and Walker 1987), and petrologic textures. This in turn should lead to further insights into processes such as inflation and lava tube formation.

Physical phenomena controlling cooling

From the veritable cornucopia of physical phenomena associated with the cooling of pahoehoe lava flows, we will show that only four processes are significant in the first few minutes. These are (a) radiative cooling at the surface, (b) atmospheric convective cooling at the surface, (c) conduction of heat within the flow including temperature and vesicle-dependent thermal properties, and (d) the release of the latent heat of crystallization.

Radiative processes

Initially, thermal radiation from the surface is the dominant heat loss mechanism from a lava flow (Fig. 3). The radiative heat flux (q_{rad}) is given by

$$q_{rad} = F\sigma_b(T_s^4 - T_a^4) \quad (1)$$

where is emissivity, F is a geometric view factor, σ_b is the Stefan Boltzmann constant, T_s is the surface temperature of the flow lobe, and T_a is the ambient temperature (e.g., Bird et al. 1960). Basaltic lavas are close to blackbodies and have emissivities which vary between 0.80 and 1.0 depending on wavelength, with 0.95

as a median value (Kahle et al. 1988; Crisp et al. 1990). For a flat plate radiating into an infinite half space, the view factor has a value of unity. Other radiative processes, such as enhanced radiation from hot cracks, radiative heat transport through the lava, and radiative heat transport across vesicles and bubbles; can be shown to be negligible (Keszthelyi 1994a, b). Although initially overwhelming, radiative heat loss is overtaken by atmospheric cooling as the lava surface cools below approximately 700 °C (Fig. 3).

Atmospheric processes

The heat flux due to atmospheric convection (q_{conv}) is typically described by the expression

$$q_{conv} = \boldsymbol{h}\ (T_s - T_a) \tag{2}$$

where $\boldsymbol{h}$ is the heat transfer coefficient, T_s is the temperature of the solid surface, and T_a is the ambient atmospheric temperature. The dimensionless Nusselt Number (Nu), the ratio of convective and conductive heat fluxes, is useful in determining $\boldsymbol{h}$. Nu is defined as

$$Nu = \boldsymbol{h}H/k \tag{3}$$

where H is the thickness of the layer of hot air and k the thermal conductivity of air.

For cooling by free convection the Nusselt Number is also given by

$$Nu = 0.225\ Ra^{1/3} \tag{4}$$

where 0.225 is an empirically determined factor and Ra is the dimensionless Rayleigh Number (Turcotte and Schubert 1982). The Rayleigh Number is defined as

$$Ra = \rho_{air}\ g\ \beta\ \Delta T\ H^3/\eta_{air}\ \kappa_{air} \tag{5}$$

where ρ_{air} is the density of the air, g is the gravitational acceleration, β the coefficient of thermal expansion of air, ΔT is the temperature difference between the ambient air and the lava surface, H is the height of the plume of hot air, η_{air} is the viscosity of the air, and κ_{air} the thermal diffusivity of air (e.g., Turcotte and Schubert 1982). Using Eqs. (3)–(5), one can solve for the free convective heat transfer coefficient ($\boldsymbol{h}_{free}$).

It is important to incorporate the temperature dependence of the atmospheric properties in these calculations. Between 700 and 30 °C, air density varies by more than a factor of three, and viscosity and thermal conductivity a factor of two. The mathematical expressions for the physical properties of air as a function of temperature are listed in Appendix A. Taking these effects into account, the free convective heat transfer coefficient is approximately 11 W/m^2 K. This value for $\boldsymbol{h}_{free}$ does not change significantly with surface temperature until the flow has cooled to near-ambient temperatures. Although trivial early on, free convection does become a nonnegligible heat loss term as the surface cools below 400 °C (Fig. 3).

Describing cooling by forced atmospheric convection (i.e., the wind) is more difficult. The forced convective heat transfer coefficient ($\boldsymbol{h}_{forced}$) cannot be accurately determined without extensive laboratory and/or numerical simulations partly because $\boldsymbol{h}_{forced}$ is very sensitive to the geometry of the problem (e.g., Bejan 1984). For example, the formula used by Head and Wilson (1986) appears applicable to lava flows on the scale of kilometers, but yields a negative $\boldsymbol{h}_{forced}$ for meter-scale lava flows. However, we were not able to find a more appropriate expression for $\boldsymbol{h}_{forced}$ in the engineering literature.

We instead attempted to apply micrometeorological models for internal thermal boundary layers (ITBL) to the cooling of pahoehoe flow lobes. An ITBL forms when air passes over a sharp change in surface temperature, such as passing from a cool lake onto a warm shore (e.g., Stunder and Sethuraman 1985; Taylor 1971). The most sophisticated ITBL models require inputs such as the stability of the atmosphere (e.g., Garratt 1990), which we were not able to measure. However, Arya (1988) does provide three readily applicable formulas:

$$q_{conv} = 2 \times 10^{-3}\ \rho_{air}\ Cp_{air}\ U\ (T_s - T_a) \tag{6}$$

$$q_{conv} = \rho_{air}\ Cp_{air}\ U\ \gamma\ H^2/(2.25\ x) \tag{7}$$

$$q_{conv} = C_H\ \rho_{air}\ Cp_{air}\ U\ (T_s - T_a) \tag{8}$$

where ρ_{air} is air density, Cp_{air} is the heat capacity of air, U is the mean wind speed, T_s is the surface temperature, T_a is the unheated air temperature, γ is the adiabatic lapse rate, H is the thickness of the ITBL, x is the downwind distance from the front of the lava, and C_H is roughly $(U^*/U)^2$, where U^* is the friction wind speed (the theoretical slip speed of the wind across the ground). The quantity (U^*/U) has been measured as approximately 0.06 at the Amboy flow field in the Mojave Desert (Greeley and Iversen 1987). The Amboy flow field consists of pahoehoe flows that are morphologically similar to those on Hawai'i. Values for our rough calculations are $\rho_{air} = 1$ kg/m^3, $Cp_{air} = 1$ kJ/kgK, and $\gamma = 0.01$ K/m. It will be shown that when measured values of the other parameters are used, Eqs. (6)–(8) seriously underestimate the convective heat flux off of lava flows (Table 2). We can only speculate that the high temperatures over lava flows drive atmospheric convection out of the regime studied by meteorologists.

Because we could find no satisfactory expression for $\boldsymbol{h}_{forced}$, we conducted a simple field experiment to constrain it. The goal of the simple field experiment was to

Table 1 Results of simple field experiment to measure cooling by wind

	T_s	T_a	ΔT	L	H	U	$\boldsymbol{h}_{forced}$
First run	450 °C	30 °C	20 °C	1 m	0.5 m	3 m/s	75 W/m^2 K
Second run	120 °C	30 °C	7 °C	6 m	1.5 m	4 m/s	70 W/m^2 K

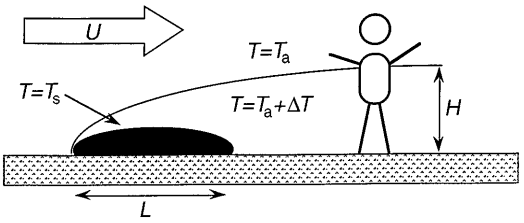

Fig. 4 Sketch of simple experiment to determine the heat transfer coefficient for forced atmospheric convection over Hawaiian pahoehoe flow lobes. This figure describes the simple field experiment carried out in March 1993 to constrain the cooling of pahoehoe lobes by the wind. By measuring the wind speed (U), thickness of the thermal boundary layer (H), and the amount by which the air within the thermal boundary layer is heated (ΔT), one can estimate the amount of heat being carried away from the lava. Although the experiment was very crude, the heat transfer coefficient was determined to within a factor of two

measure the terms in Eq. (2) to solve for $\boldsymbol{h}_{\text{forced}}$. Measuring the surface (T_s) and ambient (T_a) temperatures was straightforward. The heat flux carried by the wind (q_{conv}) was determined by measuring how much air was heated to what degree as it passed over an active flow lobe. Mathematically,

$$q_{\text{conv}} = \rho_{\text{air}} Cp_{\text{air}} U H \Delta T / L \quad (9)$$

where ρ_{air} is the density of the air, Cp_{air} is the heat capacity of the air, U is the wind velocity, H is the height of the thermal boundary layer, ΔT is the amount by which the air in the thermal boundary layer was heated above ambient, and L is the fetch over the lava flow.

Figure 4 sketches how the field experiment was carried out to measure the factors in Eq. (9). A hand-held thermoanemometer was used to measure air temperature and wind speed while a 1.6-mm-diameter K-type thermocouple was used to measure surface temperatures. The height of the thermal boundary layer was determined by finding the lowest height at which the thermometer consistently found the air temperature to be essentially ambient. Smoke grenades were used to visualize the airflow in order to help locate the boundary layer. This experiment was carried out successfully twice in March of 1993, and the measurements are tabulated in Table 1. $\boldsymbol{h}_{\text{forced}}$ was estimated as approximately 70 ± 25 W/m^2 K. This is consistent with the general rule of thumb that forced atmospheric convection is often approximately five times more efficient than free convection. It is interesting that the value for $\boldsymbol{h}_{\text{forced}}$ appears similar for runs with the lava surface at 120 and 450 °C, suggesting that $\boldsymbol{h}_{\text{forced}}$ has only a weak dependence on surface temperature. This is not surprising because previous workers have used $T^{1/3}$ or $T^{1/4}$ (e.g., Griffiths and Fink 1992a) to describe the temperature dependence for $\boldsymbol{h}_{\text{forced}}$.

Table 2 Comparison between micrometeorological models and field measurements of cooling by wind

	Measured	Eq. (6)	Eq. (7)	Eq. (8)
q_{conv} (W/m^2)				
First run	30000	2500	3	4500
Second run	7000	700	7	1300
$\boldsymbol{h}$ (W/m^2 K)				
First run	75	6	0.008	11
Second run	70	8	0.07	14

Despite the retrieval of a reasonable heat transfer coefficient, there are a great many deficiencies in this crude field experiment. Perhaps most significant is that we were not able to determine the dependence of the heat transfer coefficient on clearly important factors such as wind speed and atmospheric density. This may be only a small problem when comparing with our lava flow cooling data which were collected under atmospheric conditions essentially identical to those during the experiments to determine $\boldsymbol{h}_{\text{forced}}$. However, it does create a difficulty in applying our results to lava flows in general. Based on the micrometeorological models, $\boldsymbol{h}_{\text{forced}}$ is expected to be directly proportional to both wind velocity and atmospheric density. However, those models severely underestimate the cooling effect of wind on lava flows (Table 2) so their applicability is questionable.

Other atmospheric heat transfer mechanisms are negligible. Heat loss from air circulating within the chill crust was computed using the results of Lai and Kulacki (1991) for convection in porous media. The heat transported by this process is found to be negligible for small flow lobes, but may be very significant for lava tubes (Keszthelyi 1995b). The evaporation of water absorbs a large amount of heat, making rain a potentially significant source of cooling. However, the boiling off of a heavy rain of 1 cm/h is only equivalent to the heat lost by thermal radiation from a surface at 300 °C. Because the surface of pahoehoe flow lobes remains well over 400 °C after 5 min of cooling, rain can be ignored initially.

Latent heat of crystallization

Whereas the crystallization of slowly cooling lava lakes is well documented (e.g., Wright et al. 1976; Wright and Okamura 1977; Cashman 1993), dynamic crystallization and glass formation in the skin of lava flows are poorly quantified. If cooling is rapid enough, the lava will chill to a glass with no crystallization and negligible release of latent heat. We use the term glass transition temperature (T_g) to denote the temperature below which the viscosity of the lava is so high that crystallization does not take place over the time scale of our modeling. A more common and precise definition of the glass transition temperature is the temperature at which the extrapolated thermodynamic properties of the glass and liquid intersect (Richet and Bottinga 1986). T_g is a strong function of the major element composition, volatile content of the melt, and cooling rate (e.g., Uhlmann 1971; Kirkpatrick 1981; Richet and Bottinga 1986).

The crystallization that does occur in a rapidly cooling lava is complicated by nonequilibrium dynamic processes. The lava can super-cool significantly before the onset of crystallization. At the base of pahoehoe lobes it has been observed that this sudden, delayed onset of crystallization releases sufficient latent heat to locally raise temperatures (Keszthelyi 1995a). Oscillating temperatures due to dynamic crystallization were predicted theoretically by Brandeis et al. (1984). These oscillations are controlled primarily by the growth rate of nucleation sites, which is expressed as a function of undercooling (Kirkpatrick 1981; Brandies and Jaupart 1987).

For the purposes of our current cooling model, we have used an extremely simple crystallization model. If the lava is cooling faster than a critical rate ($\partial T/\partial t_{\text{glass}}$), no crystallization takes place. If the lava temperature is below T_g, again no crystallization takes place. If the lava is cooling slow enough and is warm enough, crystallization is modeled after the lava lake data. The volume fraction crystals (X_{cryst}) increases linearly with cooling such that

$$\partial X_{\text{cryst}}/\partial t = (\partial X_{\text{cryst}}/\partial T)\ (\partial T/\partial t) \tag{10}$$

where $\partial X_{\text{cryst}}/\partial T$ is taken to be a constant (0.5 vol% per degrees Celsius) which is the approximate mean value from lava lakes (Wright et al. 1976; Wright and Okamura 1977). The critical cooling rate, $\partial T/\partial t_{\text{glass}}$, is poorly known for Hawaiian basalts, but studies on lunar basalts suggest values on the order of 1–100 °C/s (e.g., Uhlmann et al. 1974, 1979). Extrapolating from the same lunar studies, a reasonable value for T_g for a thoeliitic basalt may be around 800–1000 °C.

Conduction

Inside the lobe heat is mostly transported by conduction. In one dimension, conduction is described by the diffusion equation:

$$\rho Cp\, \partial T/\partial t = \partial/\partial z\, (k\, \partial T/\partial z) \tag{11}$$

where z is the distance away from the cooling surface and ρ, Cp, and k are, respectively, the density, heat capacity, and thermal conductivity of the lava. Density and heat capacity of lava, as a function of temperature, is relatively well known (e.g., Murase and McBirney 1973; Touloukian et al. 1989) and can easily be corrected for vesicularity (Keszthelyi 1994b).

Thermal conductivity, on the other hand, is less well constrained. There are contradictory laboratory data that show thermal conductivity of basalt decreasing (Touloukian et al. 1989) or increasing (Cermak and Rybach 1982; Robertson 1988) with temperature. We have chosen to use a thermal conductivity that increases with temperature because these values are consistent with the behavior of glasses (e.g., Birch and Clark 1940) and lava lake cooling models (e.g., Peck et al. 1977). We have corrected thermal conductivity for the insulating effect of bubbles and vesicles (Keszthelyi 1994b). Cracks can also greatly reduce thermal conductivity (Horai 1991), but cooling-induced fracturing is not significant in the first few minutes of cooling. The expressions used for the temperature-dependent thermal properties of Hawaiian pahoehoe lobes are listed in Appendix A.

Other processes

Of the heat transport processes we have excluded from our cooling model, the motion of the lava within a flowing pahoehoe lobe requires the most justification. The heating by the advection of lava (Q_{adv}) is given by

$$Q_{\text{adv}} = \rho Cp\, \partial T/\partial t = \rho Cp\, v_x\, \partial T/\partial x \tag{12}$$

where ρ is the density of the lava, Cp the heat capacity, T the temperature, t is time, and v_x is the flow speed in the x direction. Upon examining Eq. (12) it should be clear that (a) large temperature gradients will only exist in the solid, stationary crust, and (b) that significant fluid motion is restricted to the isothermal, molten part of the flow lobe. Thus, the product of velocity and temperature gradient is essentially zero in most of the lobe.

However, near the stretching, incandescent tear in the skin of a lobe, advective heat fluxes are very large. At this tear temperature gradients as high as 1000 °C/cm are reasonable and flow velocities are typically a few centimeters per second. Thus $\partial T/\partial t$ should be locally as high as a few thousand degrees Celsius per second. Such a high advective heat flux is necessary if any incandescent material is to be exposed. However, typically, any given piece of lava remains in the vicinity of the tear for less than 10 s. Thus, we can legitimately ignore advection, except for the first few seconds around tearing sections of the crust. Also, as the heat flux out of the lava flow drops on longer time scales (hours to days), the advected heat should become relatively more significant.

Using Eqs. (3)–(5), along with values appropriate for basaltic lava, it can be shown that very little heat is transported by free convection of the molten lava within stagnant lobes. Viscous dissipation inside flow lobes produces a heating rate of on the order of only 10^{-3} °C/s (Keszthelyi 1994a). The exsolution and escape of magmatic gasses from Hawaiian basalts should have no significant direct thermal effects simply because the gasses make up such a small mass fraction of the lava (typically <0.5 wt%; Greenland 1987).

Thermal model

The above analysis of the physical processes acting on pahoehoe flows leads us to approximate the initial cooling of real pahoehoe flow lobes with a stagnant, level surface that cools via thermal radiation and atmo-

spheric convection while heat is transported internally by conduction and latent heat is added during crystallization. For short time scales, where the thermal boundary layer is much thinner than the horizontal scale of the flow lobe, the problem reduces to one spatial variable (i.e., depth). The temperature and vesicle dependence of the thermal properties and a simple crystallization model are included. The lobe is assumed to be sufficiently thick to ignore cooling from the bottom during the model run. Also, it is assumed that the heat flux at the tear in the lobe is so high that the flow starts to cool from an initially uniformly hot state. Mathematically, the problem being solved is

$$\rho Cp\,\partial T/\partial t = \partial/\partial z\,(k_{\text{eff}}\partial T/\partial z) + \rho L\,\partial X_{\text{cryst}}/\partial t \tag{13}$$

$$q_{\text{top}} = q_{\text{rad}} + q_{\text{conv}} = k_{\text{eff}}(z=0,t)\left.\frac{\partial T}{\partial z}\right|_{z=0} \tag{14}$$

$$\frac{\partial T}{\partial z}(z=Z,t) = 0 \tag{15}$$

$$T(z, t=0) = T_{\text{o}} \tag{16}$$

where T is temperature; z depth; t time; ρ, Cp, and k_{eff} are the temperature and porosity dependent density, heat capacity, and effective thermal conductivity of the lava; L is latent heat, $\partial X_{\text{cryst}}/\partial t$ is the rate of crystallization; q_{top} is the heat flux at the surface; q_{rad} is the radiative heat flux; q_{conv} is the atmospheric convective heat flux; Z is the depth to the bottom of the model; and T_{o} is the initial temperature. q_{rad} and q_{conv} are calculated using Eqs. (1) and (2), respectively. The expressions used to describe the temperature and porosity dependence of ρ, Cp, and k_{eff} are listed in Appendix A.

Because of the nonlinearity of the upper boundary condition, this set of equations must be solved numerically. A simple, fully explicit, finite-difference algorithm is used with 500 grid points spaced 0.1 mm apart and time steps of 1 ms. Small time steps are necessary because of the rapidly changing surface temperature. This drives the grid spacing to small values in order to maintain numerical stability. This in turn requires that all computations be done in 8-byte arithmetic to keep round-off errors negligible. The temperature-dependent properties are evaluated at every time step and grid point.

The basic algorithm was checked using two runs with upper boundary conditions where analytical solutions exist: $T(z=0,t) = T_{\text{a}}$ and $q_{\text{top}} = \boldsymbol{h}(T_{\text{s}} - T_{\text{a}})$ (Carslaw and Jaeger 1959). The numerical solutions converged to the analytical solution in less than 100 time steps.

Comparison to field measurements

The real test of the numerical model is its comparison with field measurements. The gentle, slow-moving character of pahoehoe flows makes obtaining field measurements from them relatively easy; thus, a significant volume of field data is available. We used three sets of field measurements from the Pu'u 'O'o–Kupaianaha eruption of Kilauea Volcano. One data set has been published in Hon et al. (1994b), and the other two were collected by the authors of this paper.

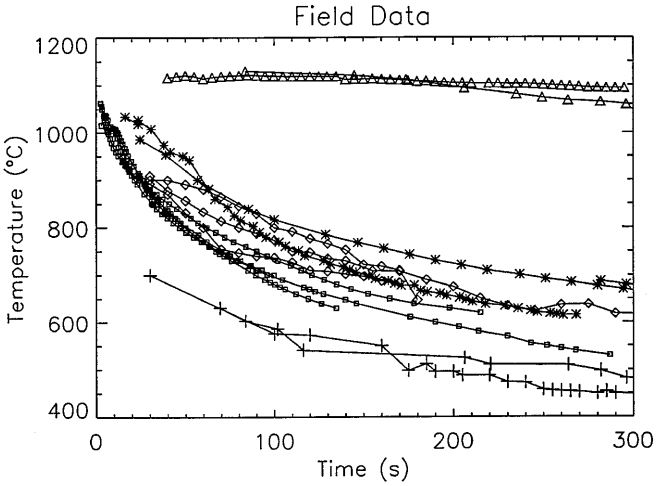

Fig. 5 Field measurements from cooling pahoehoe flow lobes. Data from Hon et al. (1994b) were collected from large sheet flows in the Kalapana area in spring 1990. Surface temperature (*crosses*) was measured with a radiometer. Measurements at ~4 mm (*asterisks*) and 2 cm (*triangles*) depth were made with sheathed K-type thermocouples (Hon et al. 1994b). 1989 measurements by R. Denlinger (*squares*) were made on the Kupaianaha flow field approximately 5 km from the lava pond. 1993 data by L. Keszthelyi (*diamonds*) were collected near the coast from the Kamoamoa flow field. 1989 measurements used fine-gauge bare thermocouples (response time <10 s) inserted 1–2 mm below the surface. 1993 data used sheathed K-type thermocouple (response time approximately 40 s) inserted 3–4 mm below the surface

The data of Hon et al. (1994b) include simultaneous measurements at several depths over a period of days. These measurements were made on pahoehoe lobes that became large sheet flows in and around the town of Kalapana in spring 1990. Surface temperatures were measured with a radiometer, whereas temperatures within the flows were measured by Cromel-Alumel (K-type) thermocouples. The reported depth of the thermocouples assumes that the probes were not bent during insertion. The thermocouples ranged from 1.6 to 6.4 mm in diameter, with the larger ones used to penetrate to depths greater than 10 cm. Temperature data from the initial cooling of three separate sheet flows are presented in Fig. 5.

We also obtained two small sets of measurements specifically for this study (Fig. 5). The first data set was collected 1–9 March 1989 approximately 5 km downslope from the Kupaianaha vent. These data consist of temperature measurements made 1–2 mm below the surface of four separate artificially induced pahoehoe flow lobes. The lobes were created by breaking open a larger flow lobe with a shovel. A fine gauge (<0.5 mm diameter), unsheathed K-type thermocouple was hooked just below the skin and allowed to freeze into the lobe. The data was recorded by videotaping the

readings from a thermocouple transducer. The lobes were collected after they had cooled in order to determine the depth to which the thermocouples had been inserted and the vesicularity of the lava. Overall, the vesicularity of the lobes was approximately 50% with vesicle distributions identical to what Walker (1989) terms spongy pahoehoe.

Our second set of measurements was made 17–19 May 1993 on the Kamoamoa Flow Field near the end of the Chain of Craters Highway. Temperatures were measured using a 1.6-mm-diameter stainless steel sheathed grounded K-type thermocouple inserted 2–3 mm into three active flow lobes. In order to reduce the heat loss through the metal sheath, the part of the thermocouple outside of the lava was covered with a ceramic insulator. The temperatures were read off of a thermocouple reader at 10- to 15-s intervals and recorded in a notebook.

The uncertainties in these field measurements are actually quite subtle. The errors attributable to the temperature sensors are minimal. At magmatic temperatures, the K-type thermocouples and thermocouple reader have an uncertainty of only $\pm 8\,^{\circ}C$ in absolute temperature and less than that for relative temperatures. Although K-type thermocouples do lose their calibration when exposed to extreme temperatures for hundreds of hours (Burley 1992), no degradation is expected on the time scale of minutes. The small diameter thermocouples we used equilibrate with the surrounding temperatures in a matter of seconds.

The significant uncertainties in the field data arise from the insertion of the thermocouples into the lava. Because of the high near-surface temperature gradients, temperatures may vary 100 °C over 1 mm. Thus, small variations in the depth of penetration into the flow are the single largest source of uncertainty. The insertion of a cooler, high thermal conductivity material into the lava also perturbs the very system we are trying to measure. However, by using small-diameter wires, these effects are minimized. The greater perturbation caused by the metal sheath vs bare wire can be seen clearly in Fig. 5.

In order to accurately model the cooling of these Hawaiian flow lobes, reasonable input values had to be selected. Based on the deepest thermocouple data from Hon et al. (1994b) and temperatures from the interior of other flow lobes, an initial lava temperature of 1135 °C was selected. The porosity for all of these flows was similar ($\sim 50\%$). We have not included the variation of vesicularity with depth in the current model. The other input parameters were 30 °C for the ambient temperature, 70 $W/m^2\,K$ for the atmospheric convective heat transfer coefficient, and 0.95 for the emissivity of the lava. The critical cooling rate to chill to a glass was taken to be 10 °C/s and the T_g to be 900 °C.

The correspondence between the model output and the field data is excellent (Fig. 6). The scatter in the field data can be explained largely by small variations in the depth of thermocouple insertion.

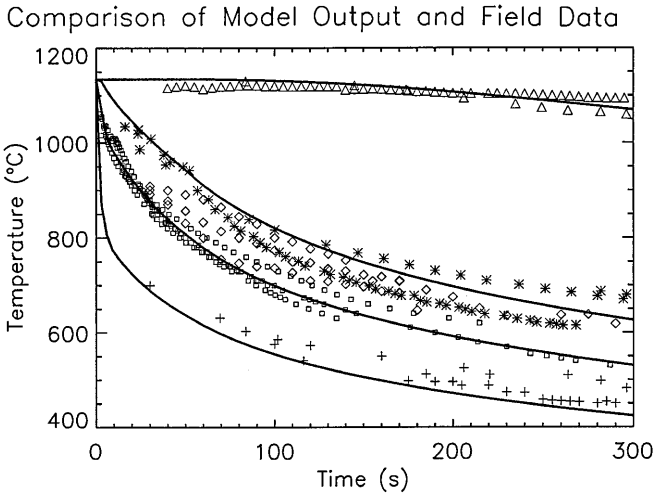

Fig. 6 Comparison of field data with model results. This figure overlays model cooling curves (*solid lines*) over all the field data. Cooling curves are plotted for the surface, 2 mm, 4 mm, and 2 cm depths. The different symbols represent data points at different depths: *crosses* surface temperatures; *squares* 1–2 mm depth; *diamonds, asterisks* 3–4 mm depth; *triangles* 2 cm depth. The thermal model was run with $T_o = 1135\,^{\circ}C$, $T_a = 30\,^{\circ}C$, $\phi = 50\%$, $h = 70$ W/m^2 K, $= 0.95$, $T_g = 900\,^{\circ}C$, $\partial T/\partial t_{glass} = 10\,^{\circ}C/s$, and included temperature- and vesicle-dependent thermal properties. The correspondence between the model and measured temperatures is excellent. This makes us confident that the model accurately represents the major physical processes involved in the initial cooling of small, slow-moving, pahoehoe lava flows

Comparison with other cooling models

The next question is whether our numerical model represents the initial cooling of pahoehoe lava flows more accurately than earlier cooling models. As previously noted, most of the earlier thermal models for lava flows cannot be applied to pahoehoe lava flows. Thus, we will compare our model results with two extremely simple analytical models, and the cooling model presented in Head and Wilson (1986) and Wilson and Head (1994). Clearly, our model also closely resembles the empirical fit to field data presented by Hon et al. (1994a), because we match the same field data.

Simple conductive cooling model

The simplest problem which resembles a cooling pahoehoe flow lobe is a slab of lava cooling by conduction as its surface is held at ambient temperature. This model should overestimate the cooling rate because the surface of a flow lobe does not instantaneously reach ambient temperatures. However, this simple model has the virtue of having an error function solution which has often been used for order of magnitude discussions about the cooling of dikes and lava flows:

$$T(z,t) = T_a + (T_o - T_a)\,\mathrm{erf}(z/\sqrt{4\kappa t}) \qquad (17)$$

where T_a is the ambient and surface temperature, T_o is the initial lava temperature, z is depth, κ is thermal dif-

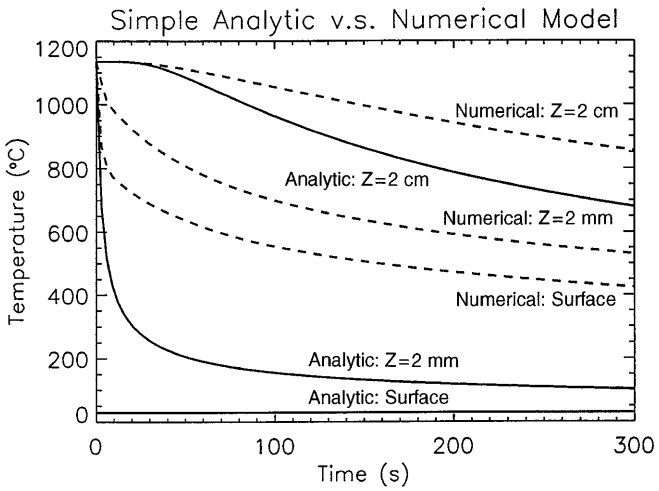

Fig. 7 Comparison between numerical model and simple analytic conductive cooling model. Simple conductive cooling model from Carslaw and Jaeger (1957) with fixed upper temperature and no latent heat- or temperature-dependent properties. Curves calculated using Eq. (17) with $T_a = 30\,°C$, $T_o = 1135\,°C$, and $\kappa = 1 \times 10^{-6}\ m^2/s$. Numerical model run for baseline case (i.e., Fig. 6). Note that this commonly used simple cooling model is very inaccurate for the initial cooling of a pahoehoe flow lobe

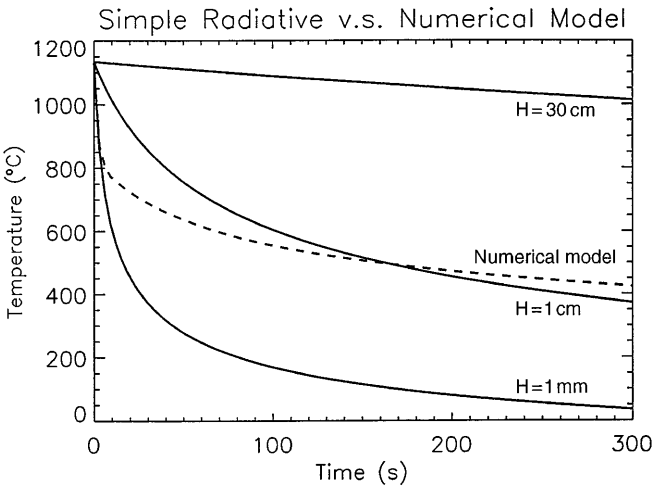

Fig. 8 Comparison between numerical model and simple radiative cooling model. Radiative cooling of an isothermal slab (Eq. (18)) with $\rho = 1300\ kg/m^3$, $Cp = 1100\ J/kg\,K$, $T_o = 1135\,°C$, and $= 0.95$. Curves plotted for slab thicknesses of 1 mm, 1 cm, and 30 cm. Numerical model run for baseline case (Fig. 6). Note that on this time scale the cooling of the lobe surface can be roughly approximated by the 1-cm-thick isothermal slab. This approximation rapidly breaks down as radiation becomes less important and the chilled crust becomes thicker

fusivity, and t is time (Carslaw and Jaeger 1959). This solution produces the well-known square root of time dependence for the growth of a chill crust. When one compares this analytic solution to our numerical model (Fig. 7) it is clear how grossly it overestimates the initial cooling of a pahoehoe flow lobe.

Simple radiative cooling model

With judicious assumptions the initial cooling of a lava surface can be better modeled as a slab cooling by radiation. In the case that the entire slab remains isothermal, a simple analytical solution exists:

$$t = \rho Cp\, H (T^{-3} - T_o^{-3}) / (3\ \ \sigma_b) \qquad (18)$$

where t is time, H is the thickness of the slab, and the other terms are defined as previously. Several workers have used this solution to build thermal models for lava flows (e.g., Danes 1972; Park and Iverson 1984; Pieri and Baloga 1986). Figure 8 plots cooling curves for various slab thicknesses. This figure shows that the assumption that the entire 30-cm-thick lobe is isothermal seriously underestimates the surface cooling rate. However, this same figure shows that one can roughly approximate the initial cooling of a pahoehoe lobe with a 1-cm-thick isothermal chill crust that cools radiatively. As the chill crust grows with time and as atmospheric cooling becomes more important, this approximation quickly breaks down.

There are more sophisticated thermal models that expand upon this simple radiative cooling model (e.g., Crisp and Baloga 1990, 1994; Gregg and Greeley 1993). For example, Crisp and Baloga (1990) divide a lava flow into a colder, fractured crust and an isothermal hot interior. This and other more complex models can theoretically achieve improved fits to the field data because they have more free parameters. However, none of these models are truly applicable to pahoehoe flows because they retain the assumption of a well-mixed interior, which is not valid for small flow lobes. Furthermore, it is important to note that these models ignore the cooling by the wind.

Cooling model of Head and Wilson (1986), Wilson and Head (1994)

The third model we compare our results to is that of Head and Wilson (1986) and Wilson and Head (1994). Head and Wilson attempt to solve exactly the same problem we have: A lava flow cooling at its top by both radiation and atmospheric convection, and heat transport in its interior by conduction including the effect of the latent heat of crystallization. Their model differs from ours only in that they ignore the temperature and porosity dependence of thermal properties. The problem with their model is that it uses analytical solutions from the case of a fixed surface temperature to estimate the cooling of the lava flow surface. Not only is this mathematically unjustifiable, but it also provides a very poor match to the field data (Table 3).

Table 3 Comparison of our cooling model and Table 1 of Head and Wilson (1986)

Surface temperature (°C)	Calculated cooling times (s)		
	Head and Wilson (1986)	Baseline model	Model with $T_0 = 1200$ °C
1200	0	—	0
1127	5.13	<0.1	0.1
1027	25.4	0.3	0.7
827	253	4.8	6.9
627	2140	55	70
427	20800	291	338

Model predictions and applications

One of the main uses of a physical cooling model is to set up controlled experiments in which parameters can be changed one at a time. These parameters can also be changed to conditions under which no active flows have been observed, such as for extraterrestrial or submarine lava flows. In the following, we examine the sensitivity of the model cooling curves to (a) lava porosity, (b) the atmospheric heat transfer coefficient, and (c) the critical cooling rate to chill to a glass. Varying other input parameters (e.g., emissivity, ambient temperature, or initial temperature) within reasonable bounds has no significant effect.

Figure 9 shows the effect of varying the porosity of the lava from 0 to 75%. After approximately 1 min, the surface of a lobe with 75% vesicularity is predicted to be more than 200 °C cooler than that of a lobe with 25% vesicles, if all other parameters are held constant. The temperature difference between the surfaces of dense lobes and vesicular lobes continues to grow slowly with time. Thus, the model suggests that there should be significant differences between the cooling histories of typical pahoehoe lobes, highly vesicular near vent lavas, vesicle-poor breakouts, and unvesiculated deep submarine lavas. Indeed, a dependence of surface cooling rate on porosity of the order of our predictions has been observed in the field for lobes between porosities of 25 and 50% (Jones 1992, 1993). However, Jones (1993) showed differences in cooling rates between flows with 23 and 28% porosity that were far larger than our model results, suggesting that parameters other than vesicularity also strongly influence the cooling rate.

Figure 10 shows the cooling curves for atmospheric convective heat transfer coefficients ($\boldsymbol{h}$) = 0, 10, 40, 70, and 100 W/m^2 K. The $\boldsymbol{h} = 0$ run demonstrates the effect of completely ignoring atmospheric convection, $\boldsymbol{h} = 10$ W/m^2 K is the minimum realistic estimate for atmospheric cooling (i.e., $\boldsymbol{h} \approx \boldsymbol{h}_{\text{free}}$), $\boldsymbol{h} = 70$ W/m^2 K is our best estimate, and $\boldsymbol{h} = 40$ and 100 W/m^2 K are about the lowest and largest values permitted by our simple field experiment. From Fig. 10 one can see that ignoring atmospheric convection in the first 5 min leads to only a small error in still air. However, after 5 min of cooling in stagnant air, a flow lobe should be 80–200 °C hotter than one cooling in a wind. Given the magnitude of this predicted effect, it is surprising that a dependence of lava surface cooling rate on wind speed has not been reported previously. It is possible that the constant (windy) weather conditions during field work on the

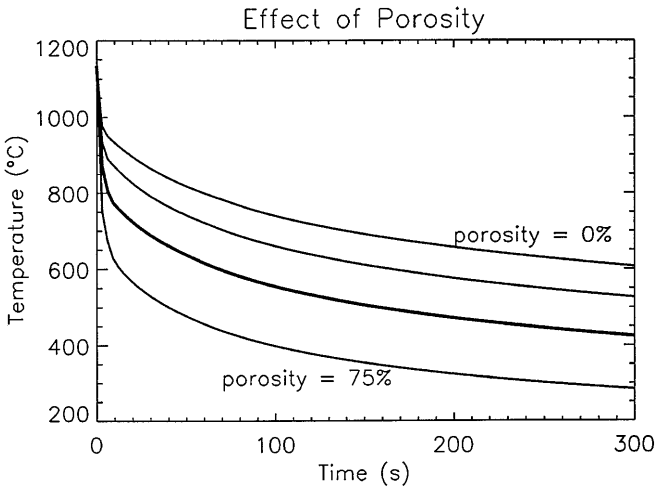

Fig. 9 Predicted effect of changing porosity. Model predictions for the surface cooling of lobes with porosities of 0, 25, 50, and 75%. Only the 0 and 75% curves have been labeled, but the effect of porosity on cooling rate is monotonic. Note that the predicted difference for the surface temperatures of lobes with 25 and 50% porosity is approximately 100 °C after 5 min of cooling, and that the temperature differences continue to grow with time

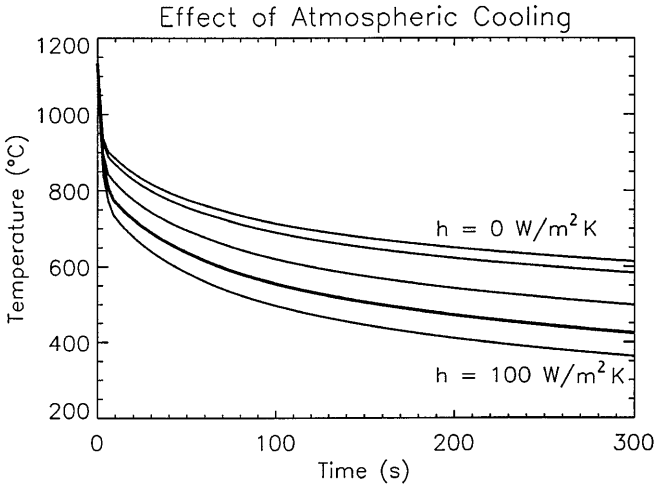

Fig. 10 Predicted effect of atmospheric convective heat transfer coefficient. Model surface cooling curves for $\boldsymbol{h} = 0$, 10, 40, 70, and 100 W/m^2 K. These runs respectively correspond to (a) no atmospheric cooling, (b) cooling in stagnant air, (c) lower limit on cooling by wind in Hawai'i, (d) nominal value for cooling by wind in Hawai'i, and (e) upper limit on cooling by wind in Hawai'i. The model predicts that there could be more than a 150 °C temperature difference between lobes cooling in stagnant air ($\boldsymbol{h} = 10$ W/m^2 K) and in a wind ($\boldsymbol{h} = 70$ W/m^2 K). This plot makes it clear that the cooling of lava flows by wind requires further investigation

Pu'u 'O'o–Kupaianaha flow field has allowed the effect of wind to be overlooked in previous field studies. It is also possible, but not likely, that $\boldsymbol{h}_{\text{forced}}$ is not sensitive to wind speed.

It would be a worthwhile and simple experiment to measure the cooling rate of pahoehoe lobes at different wind speeds, requiring no more than a radiometer, an anemometer, and patience. It may also be desirable to conduct more controlled experiments with an artificially heated plate. In any case it is clear that modeling the cooling of pahoehoe flows on the time scale of hours requires a better characterization of the convective heat transfer coefficient between lava flows and the atmosphere.

The effect of changing the critical cooling rate to chill to a glass ($\partial T/\partial t_{\text{glass}}$) from 100 °C/s (essentially complete crystallization) to 1 °C/s (little crystallization) has surprisingly little effect on surface temperatures (Fig. 11). However, at intermediate values of $\partial T/\partial t_{\text{glass}}$, there is a distinct "kink" in the cooling curve when crystallization sets in. In our model this kink takes place at approximately 10 s of cooling for $\partial T/\partial t_{\text{glass}} = 10$ °C/s. A more careful search for kinks in surface cooling curves may provide key information on the dynamic crystallization inside pahoehoe lobes.

$\partial T/\partial t_{\text{glass}}$ also controls the thickness of the glassy rind (Fig. 12). For $\partial T/\partial t_{\text{glass}} = 100$ °C/s, essentially no glass forms. At $\partial T/\partial t_{\text{glass}} = 1$ °C/s, our model predicts that a glassy rind 1–1.5 cm thick is incompletely formed after 5 min of cooling. For our nominal value of $\partial T/\partial t_{\text{glass}} = 10$ °C/s, we predict a glassy layer only 1–3 mm thick with a sharp boundary. This is only partially consistent with a preliminary petrological examination of the chilled margins of pahoehoe flow lobes. In hand sample, the glassy rind from the lobes we studied appear to be of the order of 5–8 mm thick. However, in thin section it is clear that only the outermost 1–3 mm is almost completely glassy. Across a depth of 2–8 mm, the lava consists of very fine microlites in a glassy matrix. These microlites increase in size and abundance inward, grading into an opaque mat of microlites and finally into the microcrystalline interior of the lobe. Our crude crystallization model does not show this gradational contact. Future work combining our cooling model with detailed petrographic examinations should allow the formulation of a more realistic dynamic crystallization model.

Clearly, there are many other future applications for an accurate cooling model of lava flows. With minor modifications, our model should also be applicable to extraterrestrial and submarine pahoehoe flows. Selecting appropriate values for atmospheric cooling is the single largest hurdle for such applications. The model has been extended to investigate the cooling of pahoehoe flows on the time scale of hours and days, where the effect of processes such as the motion of the lava under the crust and rain should become detectable. This cooling model can also be made applicable to the cooling of more silicic lava flows and emplaced pyro-

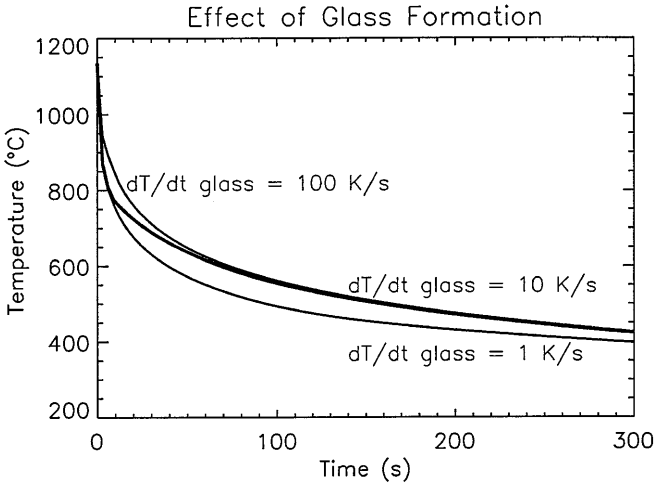

Fig. 11 Predicted effect of different critical cooling rates ($\partial T/\partial t_{\text{glass}}$). Model surface cooling curves for $\partial T/\partial t_{\text{glass}} = 1$, 10, and 100 °C/s plotted. For $\partial T/\partial t_{\text{glass}} = 100$ °C/s, almost no glass forms and the surface cools slowly. For $\partial T/\partial t_{\text{glass}} = 1$ °C/s very little crystallization takes place and the surface cools faster. For the nominal, $\partial T/\partial t_{\text{glass}} = 10$ °C/s case, there is a sharp kink as crystallization sets in and the surface crosses from the no-crystallization to the full-crystallization cooling curve. Such a kink is difficult to see in our current data set, but may be observable in the 1989 data set or in future field measurements

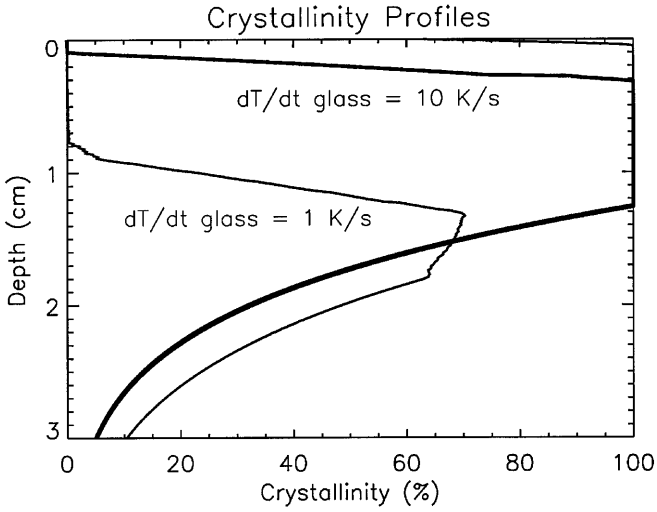

Fig. 12 Predicted effect of different $\partial T/\partial t_{\text{glass}}$ on crystallinity. Model crystallinity profiles at the end of 300 s of cooling plotted for $\partial T/\partial t_{\text{glass}} = 1$, 10, and 100 °C/s. For the $\partial T/\partial t_{\text{glass}} = 100$ °C/s case, only the uppermost 0.5 mm contains any glass. For the nominal $\partial T/\partial t_{\text{glass}} = 10$ °C/s case the glassy rind is 1–3 mm thick. In the $\partial T/\partial t_{\text{glass}} = 1$ °C/s case, pure glass extends down to 8 mm depth, and no part of the lobe has completely crystallized after 300 s of cooling. Note also that the crystallization fronts for the $\partial T/\partial t_{\text{glass}} = 100$ °C/s and $\partial T/\partial t_{\text{glass}} = 10$ °C/s cases are essentially identical by this time, with melt and crystals coexisting below 1.3 cm. In the $\partial T/\partial t_{\text{glass}} = 1$ °C/s case the reduced latent heat has led to deeper cooling of the lobe and more extensive crystallization at depths below 2 cm. Although our simple crystallization model is not able to precisely reproduce the petrographic textures seen in real lobes, it does show that combining this cooling model with a more complete dynamic crystallization model may have valuable results

clastic flows, given appropriate values for the thermal properties of those materials.

Conclusions

We have presented a new thermal model for the first 5 min of cooling of pahoehoe lava flow lobes. The model includes cooling of the surface by both thermal radiation and atmospheric convection. In the interior of the lobe we include conductive heat transport, with temperature and porosity-dependent thermal properties, and the release of the latent heat of crystallization. This model is able to accurately reproduce field measurements collected by ourselves and others.

The model is used to make some predictions about the cooling rates of pahoehoe flows under different conditions. We find that while thermal radiation is the dominant initial heat loss mechanism, atmospheric convective cooling cannot be ignored, even in the first 5 min of cooling. By the end of 5 min, the cooling by wind should be greater than cooling via thermal radiation. However, atmospheric convective cooling is poorly constrained. It was necessary to conduct a simple field experiment in order to crudely estimate the forced atmospheric convective heat transfer coefficient. More research, especially in the form of field experiments, is needed to better quantify this important parameter.

The model also predicts that the cooling of pahoehoe flows is quite sensitive to the lava porosity. A dependence of surface cooling rate on lava porosity has indeed been observed (Jones 1992, 1993). With minor alterations the model can also be used to study submarine and extraterrestrial lava flows. With more significant improvements, the model could be used to study the cooling of pahoehoe lava flows over the time scale of hours and days. Such an improved model would be a key tool in better understanding major emplacement processes of pahoehoe lava flows such as inflation and tube formation.

Acknowledgements We thank the staff of the United States Geological Survey's Hawaiian Volcano Observatory for their logistical and computer support. This work benefited greatly from discussions with James Kauahikaua, Margaret Mangan, Tari Mattox, Christina Heliker, Alun Jones, and Joy Crisp, and the extensive comments from Ken Hon and Harry Pinkerton. We thank James Foster, Jean Hsieh, and Bruce Murray for their assistance with the field work.

Appendix A

Temperature- and porosity-dependent thermal properties

This appendix provides the mathematical expressions that were used to describe the temperature- and porosity-dependent thermal properties used in the numerical model and in other discussions in this paper. The formulae below are best fits to data from the various sources. In some cases the fits are given in the reference cited, and in other cases, are computed ourselves. The data cover temperatures from 300–1000°K in detail, but for some properties data is sparse between above 1000°K. All temperatures are in Kelvins.

Gas phase

For the gas phases the properties of water vapor were used for the magmatic gas inside the bubbles in the lava because H_2O makes up approximately 80 mol% of the gasses released by Kilauea Volcano (Gerlach 1986). Model runs were made using the properties for CO_2 instead of H_2O and the resulting differences are minimal.

$$\eta_{\mathrm{gas}}(T) = \frac{a_{\mathrm{o}}\sqrt{T}}{1 + \frac{a}{T}10^{(a_1/T)}}$$

water vapor	air
$(373\,^{\circ}\mathrm{K} < T < 873\,^{\circ}\mathrm{K})$	$(79\,^{\circ}\mathrm{K} < T < 1845\,^{\circ}\mathrm{K})$
$a_{\mathrm{o}} = 1.501 \times 10^{-6}\,\mathrm{Pa\,s\,K^{-1/2}}$	$a_{\mathrm{o}} = 1.488 \times 10^{-6}\,\mathrm{Pa\,s\,K^{-1/2}}$
$a = 446.8\ \mathrm{K}^{-1}$	$a = 122.1\ \mathrm{K}^{-1}$
$a_1 = 0$	$a_1 = 5$

(Kestin, 1957)

$$\rho_{\mathrm{H_2O}}(T) \cong 222.2/T \quad (\mathrm{kg/m^3})$$
$$\rho_{\mathrm{air}}(T) \cong 352.6/T \quad (\mathrm{kg/m^3})$$
$$Cp_{\mathrm{H_2O}}(T) \cong 1860 + 1.32 \times 10^{-2}T + 4.36 \times 10^{-4}T^2 \quad (\mathrm{J/kg\,K})$$
$$Cp_{\mathrm{air}}(T) \cong 947 + 0.191\,\mathrm{T} \quad (\mathrm{J/kg\,K}) \quad \text{(Hilsenrath, 1957).}$$

The thermal conductivity of the gas phase (k_{gas}) was estimated using

$$k_{\mathrm{gas}}(T) = h_{\mathrm{gas}}(T)\ (Cp_{\mathrm{gas}}(T) + 5R/4M)$$

where R is the ideal gas constant and M is the mean atomic mass of the gas (Bird et al. 1960).

Solid and melt phases

The effective thermal conductivity (k_{eff}) of the lava combines the effect of conduction (k_{cond})and radiation across vesicles (k_{rad}):

$$k_{\mathrm{eff}} = k_{\mathrm{cond}} + k_{\mathrm{rad.}}$$

k_{rad} is very small for normal pahoehoe lobes, but is included for completeness:

$$k_{\mathrm{rad}} = 3\,\phi r \quad \sigma_{\mathrm{b}}\,T^3$$

where ϕ is the vesicularity, r is radius of the vesicle (~ 0.5 mm), $=$emissivity, σ_{b} is the Stefan Boltzmann constant, and T is the mean temperature in the vesicle (Keszthelyi 1994b).

The bulk thermal conductivity of the vesicular basalt is calculated using Maxwell's formula, which was derived for a homogeneous matrix with randomly distri-

buted spherical inclusions. Maxwell's formula is given by

$$k_{\text{cond}} = \frac{k_{\text{bas}}[2(1-\phi)\,k_{\text{bas}} + (1+2\phi)\,k_{\text{gas}}]}{[(2+\phi)\,k_{\text{bas}} + (1-\phi)\,k_{\text{gas}}]}$$

where k_{bas} and k_{gas} are the temperature-dependent thermal conductivities of the pure basalt and gas phase respectively (Robertson and Peck 1974). As mentioned previously, we have used the thermal conductivity of water vapor for k_{gas}. For the thermal conductivity of dense basalt we used

$$k_{\text{bas}}(T) = 0.848 + 1.1 \times 10^{-3}\,\text{T} \quad \text{(W/mK)}$$

(Birch and Clark 1940).

For the density of the basalt the following fit to the data from Touloukian et al. (1989) for vesicular basalt was used:

$$\rho_{\text{bas}} = \rho_{\text{o}}/(1 + \beta(T\text{-}1450))$$

where is ρ_{o} the density of dense basalt at 1450°K (ca. 2600 kg/m^3) and β is the coefficient of volumetric thermal expansion for vesicular basalt (ca. 1.5×10^{-5} K^{-1}). Touloukian et al. (1989) also provided the following expression for the heat capacity of dense basalt in units of J/kg K:

$$Cp_{\text{bas}} = \begin{cases} 1100 & \text{for } T > 1010\,\text{°K.} \\ 1211 - (1.12 \times 10^5/T) & \text{for } T \le 1010\,\text{°K.} \end{cases}$$

A value of 100 Pa s was used for viscosity in the discussions involving the flow of lava.

References

Appelgate B, Embley RW (1992) Submarine tumuli and inflated tube-fed lava flows on Axial Volcano, Juan de Fuca Ridge. Bull Volcanol 54:477–458

Arya SPS (1988) Introduction to micrometeorology. Academic Press, Orlando, pp 1–307

Ballard RD, Holcomb RT, Andel TH (1979) The Galapagos Rift at 86°W. 3. Sheet flows, collapse pits, and lava lakes of the rift valley. J Geophys Res 84:5407–5422

Basaltic Volcanism Study Project (1981) Basaltic volcanism on the terrestrial planets. Pergamon Press, New York, pp 1–1286

Bejan A (1984) Convection heat transfer. Wiley, New York, pp 1–477

Birch F, Clark H (1940) The thermal conductivity of rocks and its dependence upon temperature and composition. Am J Sci 238:529–558

Bird RB, Stewart WE, Lightfoot EN (1960) Transport phenomena. Wiley, New York, pp 1–780

Brandeis G, Jaupart C (1987) The kinetics of nucleation and crystal growth and scaling laws for magmatic crystallization. Contrib Mineral Petrol 96:24–34

Brandeis G, Jaupart C, Allegre CJ (1984) Nucleation, crystal growth, and the thermal regime of cooling magmas. J Geophys Res 89:10161–10177

Bruno BC, Taylor GJ, Rowland SK, Lucey PG, Self S (1992) Lava flows are fractals. Geophys Res Lett 19:305–308

Bryan WB, Humphris SE, Thompson G, Casey JF (1994) Comparative volcanology of small axial eruptive centers in the MARK area. J Geophys Res 99:2973–2984

Burley NA (1992) Nicrosil/Nisil Type N thermocouple. Omega complete temperature measurement handbook and encyclopedia. 28:Z33–Z36

Carrigan CR, Schubert G, Eichelberger JG (1992) Thermal and dynamical regimes of single- and two-phase magmatic flow in dikes. J Geophys Res 97 (17): 377–392

Carslaw HS, Jaeger JC (1959) Conduction of heat in solids. Oxford University Press, Oxford, pp 1–510

Cashman KV (1993) Relationship between plagioclase crystallization and cooling rate in basaltic melts. Contrib Mineral Petrol 113:126–142

Cermak V, Rybach L (1982) Thermal properties in physical properties of rocks. In: Hellwege KH (ed) Landolt-Bornstein numerical data and functional relationships in science and technology. Springer, Berlin Heidelberg New York, pp 9543–9552

Crisp J, Baloga S (1990) A model for lava flows with two thermal components. J Geophys Res 95:1255–1270

Crisp J, Baloga S (1994) Influence of crystallization and entrainment of cooler material on the emplacement of basaltic aa lava flows. J Geophys Res 95:1255–1270

Crisp J, Kahle AB, Abbott EA (1990) Thermal infrared spectral character of Hawaiian basaltic glasses. J Geophys Res 95 (21): 657–669

Danes ZF (1972) Dynamics of lava flows. J Geophys Res 77:1430–1432

Delaney PT (1988) Fortran-77 programs for conductive cooling of dikes with temperature-dependent thermal-properties and heat of crystallization. Comput Geosci 14:181–212

Flynn LP, Mouginis-Mark PJ (1992) Cooling rate of an active Hawaiian lava flow from nighttime spectroradiometer measurements. Geophys Res Lett 19:1783–1786

Garrat JR (1990) The internal boundary layer: a review. Boundary Layer Meterol 50:171–203

Gerlach TM (1986) Exsolution of H_2O, CO_2, and S during eruptive episodes at Kilauea Volcano, Hawaii. J Geophys Res 91 (12): 177–185

Greeley R, Iversen JD (1987) Measurements of wind and friction speeds over lava surfaces and assessment of sediment transport. Geophys Res Lett 14:925–928

Greenland, LP (1987) Hawaiian eruptive gases. In: Decker RW, Wright TL, Stauffer PH (eds), USGS Prof Pap 1350, pp 759–770

Gregg TKP, Fink JH (1995) Quantification of submarine lava-flow morphology through analog experiments. Geology 23:73–76

Gregg TKP, Greeley R (1993) Formation of Venusian canali: considerations of lava types and their thermal behaviors. J Geophys Res 98 (10): 873–882

Griffiths RW, Fink JH (1992a) Solidification and morphology of submarine lavas: a dependence on extrusion rate. J Geophys Res 97 (19): 729–737

Griffiths RW, Fink JH (1992b) The morphology of lava flows in planetary environments: predictions from analog experiments. J Geophys Res 97 (19): 739–748

Hardee HC (1980) Solidification in Kilauea Iki Lava lake. J Volcanol Geotherm Res 7:211–223

Head JW, Wilson L (1986) Volcanic processes and landforms on Venus: theory, predictions, and observations. J Geophys Res 91:9407–9446

Hilsenrath J (1957) Thermodynamic properties of gases. In: Gray DE (ed) American Institute of Physics Handbook. McGraw-Hill, New York, pp 4/80–4/117

Holcomb RT (1987) Eruptive history and long-term behavior of Kilauea Volcano. In: Decker RW, Wright TL, Stauffer PH (eds) Volcanism in Hawaii. USGS Prof Pap 1350, pp 261–350

Hon K, Kauahikaua J (1991) The importance of inflation in the formation of pahoehoe sheet flows. AGU Fall Meeting Abstracts, EOS 72:557

Hon K, Kauahikaua J, Denlinger R, McKay K (1994a) Emplacement and inflation of pahoehoe sheet flows: observations and measurements of active lava flows on Kilauea Volcano, Hawaii. Geol Soc Am Bull 106:351–370

Hon K, Kauahikaua J, McKay K (1994b) Inflation and cooling data from pahoehoe sheet flows on Kilauea Volcano. USGS Open-File Report 93–342B, 3.5" diskette

Horai K (1991) Thermal conductivity of Hawaiian basalt: a new interpretation of Robertson and Peck's data. J Geophys Res 96:4125–4132

Jones AC (1992) Remote sensing and thermal modelling of active lava flows, Kilauea Volcano, Hawaii. Thesis, Lancaster University, Lancaster, pp 1–288

Jones AC (1993) The cooling rates of pahoehoe flows: the importance of lava porosity. Lunar Planet Sci Conf (abstracts) XXIV: 731–732

Kahle AB, Gillespie AR, Abbott EA, Abrams MJ, Walker RE, Hoover G, Lockwood JP (1988) Relative dating of Hawaiian lava flows using multispectral thermal infrared images: a new tool for geologic mapping of young volcanic terranes. J Geophys Res 93 (15): 239–251

Kestin J (1957) Viscosity of gases. In: Gray DE (ed) American Institute of Physics Handbook. McGraw-Hill, New York, pp 2/201–2/210

Keszthelyi LP (1994a) On the thermal budget of Pahoehoe lava flows. Thesis, California Institute of Technology, Pasadena, pp 1–269

Keszthelyi L (1994b) Calculated effect of vesicles on the thermal properties of cooling basaltic lava flows. J Volcanol Geotherm Res 63:257–266

Keszthelyi L (1995a) Measurements of the cooling at the base of pahoehoe flows. Geophys Res Lett 22:2195–2198

Keszthelyi L (1995b) A preliminary thermal budget for lava tubes on the earth and planets. J Geophys Res 100 (20): 411–420

Kirkpatrick RJ (1981) Kinetics of crystallization of igneous rocks. In: Lasaga AC, Kirkpatrick RJ (eds) Kinetics of geochemical processes. Mineral Soc Am pp 321–398

Lai FC, Kulacki FA (1991) Experimental study of free and mixed convection in horizontal porous layers locally heated from below. Int J Heat Mass Transfer 34:525–541

Lockwood JP, Lipman PW (1987) Holocene eruptive history of Mauna Loa Volcano. In: Decker RW, Wright TL, Stauffer PH (eds) Volcanism in Hawaii. USGS Prof Pap 1350, pp 509–536

Mattox T, Heliker C, Kauahikaua J, Hon K (1993) Development of the 1990 Kalapana Flow Field, Kilauea Volcano, Hawaii. Bull Volcanol 55:407–413

Murase T, McBirney AR (1973) Properties of some common igneous rocks and their melts at high temperatures. Geol Soc Am Bull 84:3563–3592

Park S, Iverson JD (1984) Dynamics of lava flow: thickness growth characteristics of steady two-dimensional flow. Geophys Res Lett 11:641–644

Peck DL (1978) Cooling and vesiculation of Alae Lava Lake, Hawaii. USGS Prof Pap 935-B, pp 1–50

Peck DL, Hamilton MS, Shaw HR (1977) Numerical analysis of lava lake cooling models. Part II. Application to Alae Lava Lake, Hawaii. Am J Sci 277:415–437

Pieri DC, Baloga SM (1986) Eruption rate, area, and length relationships for some Hawaiian lava flows. J Volcanol Geotherm Res 30:29–45

Pinkerton H, Wilson L (1994) Factors controlling the lengths of channel-fed lava flows. Bull Volcanol 56:108–120

Richet P, Bottinga Y (1986) Thermochemical properties of silicate glasses and liquids: a review. Rev Geophys 24:1–25

Robertson EC (1988) Thermal properties of rocks. US Geol Surv Open-File Rep 88–441, 106 pp

Robertson EC, Peck DL (1974) Thermal conductivity of vesicular basalt from Hawaii. J Geophys Res 79:4875–4888

Rowland SK, Walker GPL (1987) Toothpaste lava: characteristics and origin of a lava structural type transitional between pahoehoe and aa. Bull Volcanol 49:631–641

Self S, Finnemore S, Thordarson Th, Walker GPL (1991) Importance of compound lava and lava-rise mechanisms in emplacement of flood basalts. AGU Fall Meeting (abstracts) Eos, 72:566

Stunder M, Sethuraman S (1985) A comparative evaluation of the coastal internal boundary-layer height equations. Boundary Layer Meteorol 32:177–204

Taylor PA (1971) Airflow above changes in surface heat flux, temperature, and roughness: an extension to include the stable case. Boundary Layer Meteorol 1:474–497

Theilig E, Greeley R (1986) Lava flows on Mars: analysis of small surface features and comparisons with terrestrial analogs. Proc Lunar Planet Sci Conf 17: 193–206

Touloukian YS, Judd WR, Roy RF (eds) (1989) Physical properties of rocks and minerals. Hemisphere Publishing Co., New York, pp 1–548

Turcotte DL, Schubert G (1982) Geodynamics. Wiley, New York, pp 1–450

Uhlmann DR (1971) A kinetic treatment of glass formation. J Non-Cryst Solids 7:337–348

Uhlmann DR, Klein L, Kritchevsky G, Hopper RW (1974) The formation of lunar glasses. Proc Lunar Planet Sci Conf 5:2317–2331

Uhlmann DR, Onorato PIK, Scherer GW (1979) A simplified model for glass formation. Proc Lunar Planet Sci Conf 10:375–381

Walker GPL (1989) Spongy pahoehoe in Hawaii: a study of vesicle-distribution patterns in basalt and their significance. Bull Volcanol 51:199–209

Wilmoth RA, Walker GPL (1993) P-type and S-type pahoehoe: a study of vesicle distribution patterns in Hawaiian lava flows. J Volcanol Geotherm Res 54:129–142

Wilson L, Head JW (1994) Mars: review and analysis of volcanic eruption theory and relationships to observed landforms. Rev Geophys 32:221–263

Wright TL, Okamura RT (1977) Cooling and crystallization of tholeiitic basalt, 1965 Makaopuhi lava lake, Hawaii. US Geol Surv Prof Pap 1004, pp 1–59

Wright TL, Peck D, Shaw H (1976) Kilauea lava lakes: natural laboratories for the study of cooling, crystallization, and differentiation of basaltic magma. In: Sutton GH, Manghnani MH, Moberly R (eds) The geophysics of the Pacific Ocean basin and its margin. Am Geophys Union Monograph 19:375–392